Meat and Muscle Biology™

Toward the Prediction of the PSE-Like Muscle Defect in Cooked Hams

Laetitia Théron[1]*, Thierry Sayd[1,2], Christophe Chambon[2], Antoine Vautier[3], Claude Ferreira[1], Laurent Aubry[1], Annie Vénien[1], Didier Viala[2], Thierry Astruc[1], Vincenza Ferraro[1], and Véronique Santé-Lhoutellier[1]

[1]INRAE, UR370 QuaPA, F-63122, Saint Genès Champanelle, France
[2]INRAE, 2018. Metabolomic and Proteomic Exploration Facility (https://doi.org/10.15454/1.557239511356972E12, F-63122), Saint Genès Champanelle, France
[3]IFIP–Institut du Porc, La motte au Vicomte, BP 35104, F-35561, Le Rheu Cedex, France
*Corresponding author. Email: laetitia.theron@inrae.fr (Laetitia Théron)

Abstract: Pale Soft Exudative (PSE)-like muscle defect is of great importance in the cooked ham industry because of the economic losses it can cause. The flagship product is the "Jambon supérieur," a polyphosphate-free cooked ham, usually sold sliced and packaged. Slicing is an automatic process that reveals the defect as holes in the slice leading to slicing losses. Up to now, the PSE-like defect has only been detected on raw meat after deboning the pork leg because it affects the inner part of the *semimembranosus* muscles and also the *adductor* muscles. The objective of this study was to develop innovative approaches that combine mechanistic elucidation and the discovery of potential biomarkers (i) at the level of the muscle and (ii) at the level of the live animal by analyzing proteins from plasma. The use of chemometrics for the spectral fingerprinting of pig plasma was chosen to predict the PSE-like muscle defect in raw hams.

Key words: PSE-like, ham, proteomic, imaging, mass spectrometry, predictive model
Meat and Muscle Biology 4(2): 13, 1–6 (2020) **doi:10.22175/mmb.11156**
Submitted 22 April 2020 Accepted 28 May 2020

This paper was accepted as a contribution to the 2020 International Congress of Meat Science and Technology and the AMSA Reciprocal Meat Conference.

Introduction

The Pale Soft Exudative (PSE)-like defect that occurs in raw meat used to produce cooked hams is a major issue. Indeed, it can represent up to 50% of the total processed ham, the French "jambon supérieur" cooked ham, and leads to significant economic losses (Vautier et al., 2008). The defect is mainly detected during the automated slicing process, by the appearance of holes within the ham slices. Because of the histological and biochemical similarities observed on muscles, this defect is compared to PSE meat, but in most cases, it is located in the deepest regions of the *semimembranosus* muscle, near the femur bone (Vautier et al., 2008). The defect finds its origin in a combination of risk factors that are associated with more than just stress or stress sensitivity, and chilling was not found to influence the defect frequency (Vautier et al., 2008).

Although previous observations have suggested a gradient within the ham (Franck et al., 1999) (indeed, the defect starts to appear on the internal surface of the *semimembranosus* and the *adductor*, then spreads out toward subcutaneous regions for strong cases without being noticeable from the outside of bone-in hams), no information is available regarding the progression of the PSE-like defect within muscles. Furthermore, because of its high variability, there is a strong need

for a discriminative sort key to classify raw material prior to ham processing. Recently, the use of near-infrared spectroscopy was proven efficient to classify fresh pork meat and to predict the suitability of fresh pork meat for the production of cooked ham (Neyrinck et al., 2015).

In this context, we first aimed to elucidate the development of the PSE-like defect by its characterization from the tissue to the molecular scale using mass spectrometry approaches. In the second part, we developed a predictive method to classify raw material prior to ham processing using blood samples, using the spectral fingerprints of plasma proteins studied by Matrix-Assisted Laser Dissociation Ionization Time-of-Flight (MALDI-TOF) mass spectrometry and Attenuated Total Reflectance-Fourier Transform InfraRed (ATR-FTIR) Spectroscopy.

Materials and Methods

Animal, muscle, and blood samples

A batch of 120 pigs (from a sow Large White × Landrace and Pietrain sire), from different farms, were slaughtered at the commercial abattoir "la Guerche de Bretagne, France." Carcasses were blast-chilled for 1 h and 15 min, and blood was collected from each animal and treated as described in the following section. At 24 h post mortem, after pH and temperature stabilization, hams were sorted according to their level of destructuration on a scale from 1 to 4 (Vautier et al., 2008), their pH, temperature, and exudate values. From the 120 animals, 20 were selected, based on the destructuration score—10 "normal hams" (NH) and 10 "PSE-like hams" (DH). The inner part (DHi) and outer parts (DHo) of *semimembranosus* muscles were sampled in each of the DH, and the inner part of *semimembranosus* muscles was sampled in each of the NH.

MALDI-TOF mass spectrometry imaging of ham samples

At 24 h post mortem, *semimembranosus* muscle samples (1 × 1 × 1 cm) were collected, positioned on a cork plate, and cryofixed by immersion at −160°C in isopentane cooled with liquid nitrogen (−196°C). Serial cross-sections (10 µm thick) were cut using a cryostat (Microm HM 560; Thermo Scientific) and were collected on glass slides for histological stains and on indium tin oxide glass slides (Bruker Daltonik, Bremen, Germany) for MALDI-mass spectrometry imaging (MSI). The glass slides were stored under vacuum until use. The muscle sections were subjected to 2 washing steps at 70% and 95% ethanol to deplete lipids and then dried in a desiccator for 30 min. The sinapinic acid matrix was 10 mg/mL in water/acetonitrile at 60:40 (v/v) with 0.2% trifluoroacetic acid, applied using ImagePrep (Bruker Daltonics) according to the manufacturer's recommendations. The spectral data were acquired on an Autoflex Speed MALDI-TOF/TOF mass spectrometer equipped with a Smartbeam laser, using FlexControl 3.4 and FlexImaging 3.0 software packages (Bruker Daltonics). Ions were detected in positive linear mode over a mass range of m/z 2,000–20,000 with a sampling rate of 0.63 GS/s. The lateral spatial resolution was set to 75 µm, and a total of 500 laser shots were accumulated per pixel at constant laser power, using random movement within each pixel. The deflection was set at an m/z of 1,500 and laser focus at medium. Analyses were performed using a detector gain of 2.69 V, ion source voltage 1 at 19.5 kV, ion source voltage 2 at 18.15 kV, and lens voltage at 7 kV. Spectral data were loaded into SCiLS Lab 2016 software (http://scils.de/; Bremen, Germany). The following workflow was used for data treatment: baseline subtraction using the TopHat algorithm, normalization by the total ion current algorithm, and peak picking using the orthogonal matching pursuit algorithm, with peak alignment and spatial denoising.

Plasma proteins spectral fingerprints by MALDI-TOF mass spectrometry and FTIR spectroscopy

Immediately after slaughter, a whole blood sample was collected from each pig in a heparinized tube (Venosafe, Terumo, Shibuya, Tokyo, Japan). After 5 stirrings, the tubes were centrifuged at 1500*g* for 10 min. The plasma was recovered and frozen immediately in liquid nitrogen. The samples were stored at −80°C until use. For the MALDI-TOF mass spectrometry protein fingerprint, plasma proteins were pre-purified using Spin Tubes (C18 Agilent Peptide Cleanup, Agilent Technologies, Wilmington, DE) according to the manufacturer's instructions. Then, 1 µl of pre-purified plasma proteins was manually spotted in triplicate on a polished steel target (MTP 384 Target Plate Polished Steel, Bruker Daltonics GmbH, Bremen, Germany) at a ratio of 1:1 with the matrix. The matrix used was α-cyano-4-hydroxycinnamic acid matrix at 7 mg/mL in water/acetonitrile 50:50 (v/v) with 0.2% trifluoroacetic acid. The mass spectrometer used to acquire the protein fingerprinting was an Autoflex Speed MALDI-TOF/TOF with a Smartbeam

laser, using FlexControl (version 3.4) software (Bruker Daltonics GmbH, Bremen, Germany). A total of 4,000 spectra were accumulated randomly per sample. The laser power was constant for all the samples, and the laser focus was set at medium. Ion detection was done in linear mode at a mass range of m/z 1,000–10,000, with a sampling rate of 0.31 GS/s. Acquisition deflection was set at m/z 1,000. The detector gain was set at 2,500 V, the ion source voltage 1 at 19.56 kV, the ion source voltage 2 at 18.11 kV, and the lens voltage at 7 kV. External calibration of spectra was done through the deposition of a protein standard (Protein Calibration Standard I, Bruker Daltonics) before each measurement on the same target. MALDI-TOF spectra were processed using FlexAnalysis software (version 3.4) (Bruker Daltonics GmbH, Bremen, Germany). Baseline subtraction using the TopHat algorithm was set with a 5% minimal baseline width. Smoothing was performed with a 1 Da width and 5 cycles. Individual spectra were normalized using the Total Ion Count (TIC) value. Peak picking was applied using the peak intensities with a signal to noise ratio of 2. Infrared spectra were obtained using a Bruker Tensor II spectrometer, and an ATR accessory with 250 µm × 250 µm diamond crystal (Specac Ltd., Orpington, UK) operated by the OPUS 7.5 software (Bruker, Bremen, Germany). The spectral resolution was set at 4 cm^{-1}, and 100 scans were used for each measurement in the range of 4,000–600 cm^{-1}. All the sample acquisitions were performed 5 times as follows: 1 µL of plasma was spotted on the diamond crystal and left to dry at room temperature for 8 min. Between samples, the ATR crystal was cleaned with deionized water and ethanol, and for each sample measurement, a background spectrum was recorded for correction. The 3 best spectra out of 5 were analyzed. After atmospheric compensation and baseline correction, the spectra were pre-processed by the second derivative operation and cropped to obtain 2 areas of interest: 1,800–900 cm^{-1} and 3,450–2,700 cm^{-1}. Each area was then normalized using vector normalization, and the mean spectra of the 3 replicates were used.

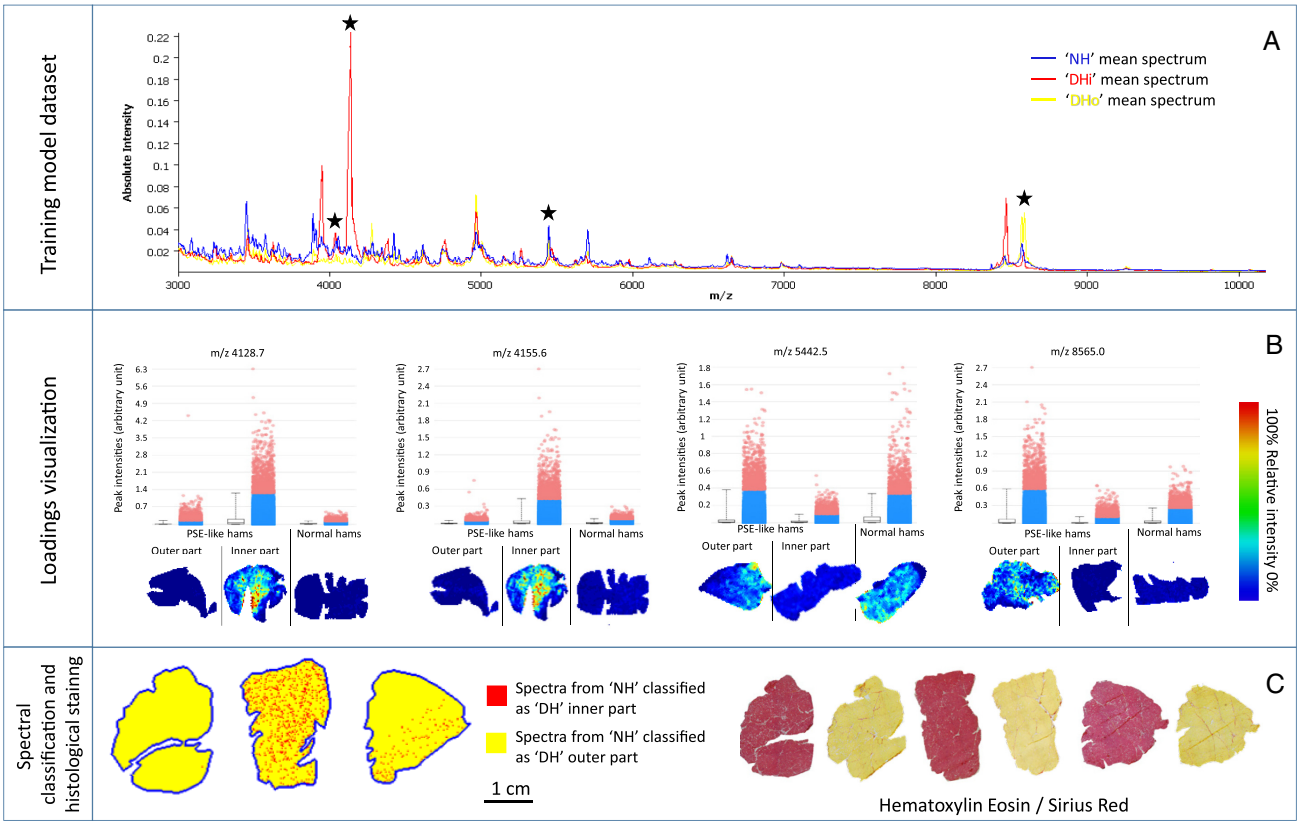

Figure 1. Predictive model of the PSE-like areas. (A) Mean spectra acquired on the muscle sections from the "normal hams" (in blue, $n = 10$), on the muscle sections from the inner (in red, $n = 10$) and outer (in yellow, $n = 10$) parts of "PSE-like hams." The peaks with the highest loading scores and biggest contribution to the predictive model are represented by stars. (B) Box plot and graphical representation of all the individual peak intensities observed on the muscle sections, and ionic map for m/z 4128.7, m/z 4155.6, m/z 5442.5, and m/z 8565.0 for representative tissue section samples from "DHo," "DHi," and "NH." (C) NH spectral data classification using the predictive model: the spectra from NH classified as DHi are shown in red, and the spectra from NH classified as DHo are shown in yellow. Serial cross sections were stained with Sirius Red to reveal the connective network and with hematoxylin and eosin to reveal the tissue structure. DHi = inner parts of PSE-like hams; DHo = outer parts of PSE-like hams; NH = normal hams; PSE = Pale Soft Exudative.

Chemometrics

Neuronal network analysis was performed using Orange software (Demsar et al., 2013). The number of neurons per hidden layer was set at 100 with an activation function by logistics. The solver parameter for weight optimization was "Adam," a stochastic gradient-based optimizer. The alpha parameter, the regularization term, was set at 0.0001, and the maximum number of iterations was set at 200. Internal validation was performed using a stratified 5-fold cross-validation. The classification results using the predictive model are given for each sample of PSE-like muscle defect (DH, $n = 6$) and normal (NH, $n = 7$) hams. The classification assignment is given (NH/DH) and shown in gray in the case of misclassification. The score probability of classification assignment is given for each class, i.e., DH and NH.

Results

Spatial variability of the DH defect

The spatial variability of the PSE-like defect that occurs in cooked hams was investigated by MSI by MALDI-TOF. To determine whether the defect progressed internally within the ham, indicating a local heterogeneity, the relationship between NH molecular maps with both DHi and DHo was studied. The training set used to build the predictive model was composed of the spectral data of the DHi and DHo. Then, the data from the NH were classified using this model to determine the class to which they were closer: DHi or DHo. The model's performance was evaluated by cross-validation accuracy, which was 87%. The model's performance can be expressed as its capability to describe

Table 1. Evaluation and results of the predictive model, using a neural network algorithm, to classify PSE-like muscle defect and normal hams

	MALDI-TOF MS spectral fingerprint		ATR-FTIR spectral fingerprint		MALDI-TOF MS and ATR-FTIR spectral fingerprints	
Evaluation results of the predictive model by neural network algorithm						
AUC	1.000		1.000		1.000	
CA	0.846		0.846		1.000	
F-1	0.840		0.844		1.000	
Precision	0.880		0.885		1.000	
Recall	0.846		0.846		1.000	
Classification results using the predictive model by neural network algorithm						
Identification	**Classification assignment**	**Score probability**	**Classification assignment**	**Score probability**	**Classification assignment**	**Score probability**
		PSE **N**		**PSE** **N**		**PSE** **N**
N17	N	0,218 0,782	PSE	0.661 0.339	N	0.011 0.989
N30	N	0,238 0,762	N	0.090 0.910	N	0.033 0.967
N41	N	0.064 0.936	N	0.013 0.987	N	0.001 0.999
N42	N	0.013 0.987	N	0.006 0.994	N	0.002 0.998
N54	N	0.015 0.985	PSE	0.969 0.031	N	0.095 0.905
N78	N	0.254 0,746	N	0.005 0.995	N	0.009 0.991
N91	N	0.385 0,615	N	0.014 0.986	N	0.013 0.987
PSE24	PSE	0.996 0.004	PSE	0.949 0.051	PSE	0.957 0.043
PSE47	PSE	0.973 0.027	PSE	0.988 0.012	PSE	0.993 0.007
PSE50	PSE	0.996 0.004	PSE	0.995 0.005	PSE	0.999 0.001
PSE68	N	0.345 0.655	PSE	0.994 0.006	PSE	0.999 0.001
PSE77	N	0.436 0,564	PSE	0.761 0.0,239	PSE	0.516 0.484
PSE80	PSE	0.999 0.001	PSE	0.629 0.371	PSE	0.999 0.001

The evaluation results of the predictive model are given for each spectral method, i.e., MALDI-MS and IR, and are expressed as AUC, CA, F-1, Precision, and Recall values (from 0 to 1). AUC is the Area under ROC, the Receiver-Operating Curve; CA is the Classification Accuracy, the proportion of correctly classified samples; F-1 is a weighted harmonic mean of precision and recall; Precision is the proportion of true positives among instances classified as positive, e.g., PSE-like hams correctly identified as PSE-like hams; and Recall is the proportion of true positives among all positive instances in the data, e.g., the number of PSE-like hams among the normal hams. The classification results using the predictive model are given for each individual sample of PSE-like muscle defect ("PSE," $n = 6$) and normal ("N," $n = 7$) hams. The classification assignment is given (N or PSE), shown in gray in the case of misclassification. The score probability of classification assignment is given for each class, i.e., PSE and N.

ATR-FTIR = Attenuated Total Reflectance-Fourier Transform InfraRed; IR = Infrared; MALDI = Matrix-Assisted Laser Dissociation Ionization; MS = Mass Spectrometry; PSE = Pale Soft Exudative; TOF = Time of Flight.

the spectral classes, in percentage, and its use as a tool to determine the class in which the new spectral data belonged. The m/z intensities on which the model's performance rely are those showing the highest scores: m/z 4128.7, m/z 4155.6, m/z 5442.5, and m/z 8565.0. These 4 peaks are represented in Figure 1A with stars on the mean spectra. The two first peaks, m/z 4128.7 and m/z 4155.6, are significantly more intense in the DHi compared with the DHo and those of the NH. This result confirmed the hypothesis according to which the structural defect is internal, and that the DHo present more similarities to the NH. Boxplots and all the individual intensities measured on each pixel are shown in Figure 1B, as well as an example of an ionic map for each ion. It appeared very clear that these two ions are co-localized and that their intensities are correlated. The mass shift of 27 Da could be due to oxidation of arginine (to glutamic acid) (https://abrf.org/delta-mass), and the oxidation product of arginine may be glutamic semialdehyde, a carbonyl that is a very well described modification in meat products (Estévez, 2011). Indeed, the carbonylation of proteins from chicken breast meat has been studied and linked to PSE meat (Estévez, 2015; Carvalho et al., 2017). Despite the absence of direct protein identification using MSI by MALDI-TOF, altogether these results could suggest that m/z 4128.7 and m/z 4155.6 are the same protein or peptide from the same protein, with the presence of an amino acid modification. The intensities plot of m/z 5442.5 was lower in the DHi, while those of m/z 8565.0 were higher in the DHo. Furthermore, the ionic map of these ions indicated that their intensities were not homogenous on the tissue section but showed spatial specificity, which could not be seen without imaging by mass spectrometry.

Then, the predictive model, mainly based on these ion intensities, was used to classify the spectral data from NH. Thanks to this approach, the spectral data from NH could be classified as being closer to the DHi or the DHo. Spectral data using this predictive model were classified for every spectrum of the sections from NH and were represented as a color map: the spectrum belonging to the DHi in red and the spectra belonging to the DHo in yellow (Figure 1C).

Table 2. Evaluation and results of the predictive model, using a neural network algorithm, to classify PSE-like muscle defect and normal ham, including all the m/z class attributes

Class	N	N	N	N	N	N	N	D	D	D	D	D	D
Identification	N17	N30	N41	N42	N54	N78	N91	PSE24	PSE47	PSE50	PSE68	PSE77	PSE80
Neural Network	N	N	N	N	N	N	N	PSE	PSE	PSE	N	N	PSE
Neural Network (D)	0.218	0.238	0.064	0.013	0.015	0.254	0.385	0.996	0.973	0.996	0.345	0.436	0.998
Neural Network (N)	0.782	0.762	0.936	0.987	0.985	0.746	0.615	0.004	0.027	0.004	0.655	0.564	0.002
m/z	**Class Attributes**												
1123.45	0.71	0.45	0.93	0.40	0.78	0.91	0.93	0.71	1.13	1.19	1.68	0.48	1.59
1141.52	0.27	0.53	0.53	0.28	0.15	0.92	0.90	0.64	1.39	1.97	0.45	0.22	2.45
1159.83	0.16	0.38	0.36	0.24	0.15	0.55	0.67	0.48	0.90	1.60	0.27	0.20	2.15
1409.07	0.29	0.30	0.54	0.20	0.14	0.55	0.53	0.32	0.79	1.26	0.51	0.20	1.47
1547.11	0.19	0.16	0.24	0.15	0.17	0.62	0.34	0.30	0.67	1.15	0.18	0.25	1.76
1623.01	0.29	0.39	0.43	0.30	0.34	0.71	0.69	0.54	1.04	1.75	0.47	0.32	2.30
1811.76	0.17	0.35	0.19	0.19	0.16	0.43	0.43	0.39	0.56	0.96	0.21	0.26	0.86
1998.73	0.48	0.62	0.73	0.46	0.70	0.66	0.63	0.71	0.71	0.85	1.06	0.48	0.97
2154.31	3.47	2.92	3.45	1.81	7.20	2.35	1.23	0.66	0.76	0.99	0.50	0.74	1.23
2239.21	0.50	0.30	0.39	0.21	0.37	0.59	0.16	0.71	0.80	0.43	0.77	0.31	0.69
2287.61	0.29	0.19	0.26	0.19	0.30	0.64	0.35	0.56	0.41	0.72	0.48	0.29	1.25
2378.15	0.61	1.41	0.50	0.59	0.96	0.80	1.34	1.43	1.25	1.24	1.38	1.08	1.33
2574.58	0.30	0.81	0.35	0.28	0.47	0.87	0.62	0.82	1.10	0.87	0.49	0.80	0.89
2701.67	0.44	0.58	0.40	0.31	0.47	0.44	0.44	0.55	0.51	0.63	0.48	0.52	0.56
3277.30	0.52	1.10	0.67	0.87	2.01	0.89	0.78	1.78	0.87	1.75	2.34	1.31	2.10
3476.56	0.66	0.16	0.29	0.20	0.37	0.45	0.33	0.61	0.37	0.49	0.44	0.79	1.49
4564.62	0.14	0.23	0.18	0.50	1.19	0.54	0.79	3.59	0.89	2.93	2.73	1.38	3.61
5182.11	0.07	0.09	0.06	0.05	0.35	0.31	0.20	0.04	0.04	0.05	0.03	0.08	0.08
5601.50	0.05	0.05	0.02	0.03	0.08	0.19	0.04	0.16	0.10	0.09	0.07	0.16	0.24
6948.88	0.89	0.11	0.30	0.44	0.51	0.72	0.56	1.29	0.54	0.54	0.97	2.49	3.40

PSE = Pale Soft Exudative.

Plasma protein fingerprint to predict the PSE-like muscle defect

The second part of the study aimed to assess the capacity of protein fingerprinting by MALDI-TOF mass spectrometry and ATR-FTIR spectroscopy to predict the PSE-like muscle defect in hams. Plasma samples were chosen since it is essential not to depreciate the carcass and to develop an easy-to-use method, blood sampling being easier than muscle biopsies. In the first part of this study, the prediction capacity of both spectral approaches was assessed separately using multivariate analysis. Then, both data matrixes were analyzed using the most discriminant spectra features to determine the synergy of both of these spectral methods. The predictive model built using neural network analysis from MALDI-TOF spectra showed a classification accuracy of 84.6% and a precision and recall of 88% and 84.6%, respectively, resulting in the correct classification of 100% of NH samples, whereas 2 DH samples were misclassified (Tables 1–2). This misclassification has to be moderated by the number of observations and by their corresponding score probability. Indeed, in both cases, the score probabilities were 56.4% and 65.5% for the DH class and 43.6% and 34.5% for the NH class. The neural network built with FTIR spectra showed a classification accuracy of 84.6% and a precision and recall of 88.5% and 84.6%, respectively. This resulted in the correct classification of 100% of DH samples, whereas 2 NH samples were identified as a false negative, classified as DH (Table 1), with a score probability of 66.1% and 96.9%.

To demonstrate the synergy of both spectral fingerprints in predicting the PSE-like muscle defect, both approaches were combined. The respective top 30 features found to be the most relevant in the neural networks obtained with MALDI-TOF and FTIR spectral fingerprints were analyzed to build a new predictive model. The results showed a classification accuracy of 100%, with a precision and recall of 100% and 100%. Thus, the classification results confirmed the relevance of such a combinatory approach since it improved the correct classification assignment up to 100%. All the individual spectra were correctly classified, meaning that the neural network successfully predicted the PSE-like muscle defect in all cases.

Conclusions

The spectral approaches used in this study have proven efficient to characterize the PSE-like muscle defect from the tissue to the molecular scales. This integrative study resulted in the definition of relevant protein markers to better understand the defect evolution within ham. Then, the spectral approaches were found to be highly discriminative in predicting PSE-like defect using a plasma sample and thus were without any depreciation of the carcass. Furthermore, this proof of concept has demonstrated the synergy of both spectral methods, thereby opening up new perspectives regarding their application in industrial conditions.

Literature Cited

Carvalho, R. H., E. I. Ida, M. S. Madruga, S. L. Martinez, M. Shimokomaki, and M. Estévez. 2017. Underlying connections between the redox system imbalance, protein oxidation and impaired quality traits in pale, soft exudative (PSE) poultry meat. Food Chem. 215:129–137. https://doi.org/10.1016/j.foodchem.2016.07.182.

Demsar, J., T. Curk, A. Erjavec, C. Gorup, T. Hocevar, M. Milutinovic, M. Možina, M. Polajnar, M. Toplak, A. Stari , M. Štajdohar, L. Umek, L. Žagar, J. Žbontar, M. Žitnik, and B. Zupan. 2013. Orange: Data mining toolbox in Python. J. Mach. Learn. Res. 14:2239–2253.

Estévez, M. 2011. Protein carbonyls in meat systems: A review. Meat Sci. 89:259–279. https://doi.org/10.1016/j.meatsci.2011.04.025.

Estévez, M. 2015. Oxidative damages to poultry: From farm to fork. Poultry Sci. 94:1368–1378. https://doi.org/10.3382/ps/pev094.

Franck, M., G. Bénard, X. Fernandez, S. Barbry, P. Durand, and H. Lagant. 1999. Observations préliminaires sur le jambon déstructuré– Description du phénomène et étude de quelques facteurs de variation. In: Journées de la Recherche Porcine, Rennes, France. 31:331–338.

Neyrinck, E., S. De Smet, L. Vermeulen, D. Telleir, S. Lescouhier, H. Paelinck, I. Fraeye, R. Geers, and K. Raes. 2015. Application of near-infrared spectroscopy for the classification of fresh pork quality in cooked ham production. Food Bioprocess Tech. 8:2383–2391. https://doi.org/10.1007/s11947-015-1583-z.

Vautier, A., J. Boulard, J. Houix, and B. Minvielle. 2008. Prediction level of meat quality criteria on “PSE-like zones” defect of pork’s ham. 54th International Congress of Meat Science And Technology (ICoMST), 7A-27, Cape Town, South Africa.